



OPEN

Strong Temporal Variation Over One Saturnian Year: From Voyager to Cassini

SUBJECT AREAS:

GIANT PLANETS

ASTRONOMY AND PLANETARY
SCIENCE

PLANETARY SCIENCE

PHYSICS

Received
22 April 2013

Accepted
22 July 2013

Published
12 August 2013

Correspondence and
requests for materials
should be addressed to
L.L. (lli7@central.uh.
edu)

Liming Li¹, Richard K. Achterberg², Barney J. Conrath³, Peter J. Gierasch³, Mark A. Smith¹, Amy A. Simon-Miller⁴, Conor A. Nixon⁴, Glenn S. Orton⁵, F. Michael Flasar⁴, Xun Jiang¹, Kevin H. Baines⁵, Raúl Morales-Juberías⁶, Andrew P. Ingersoll⁷, Ashwin R. Vasavada⁵, Anthony D. Del Genio⁸, Robert A. West⁵ & Shawn P. Ewald⁷

¹University of Houston, Houston, TX, ²Department of Astronomy, University of Maryland, College Park, MD, ³Department of Astronomy, Cornell University, Ithaca, NY, ⁴NASA Goddard Space Flight Center, Greenbelt, MD, ⁵Jet Propulsion Laboratory, California Institute of Technology, Pasadena, CA, ⁶Physics Department, New Mexico Institute of Mining and Technology, Socorro, NM, ⁷Division of Geological and Planetary Sciences, Caltech, Pasadena, CA, ⁸NASA Goddard Institute for Space Studies, New York, NY.

Here we report the combined spacecraft observations of Saturn acquired over one Saturnian year (~29.5 Earth years), from the Voyager encounters (1980–81) to the new Cassini reconnaissance (2009–10). The combined observations reveal a strong temporal increase of tropic temperature (~10 Kelvins) around the tropopause of Saturn (i.e., 50 mbar), which is stronger than the seasonal variability (~a few Kelvins). We also provide the first estimate of the zonal winds at 750 mbar, which is close to the zonal winds at 2000 mbar. The quasi-consistency of zonal winds between these two levels provides observational support to a numerical suggestion inferring that the zonal winds at pressures greater than 500 mbar do not vary significantly with depth. Furthermore, the temporal variation of zonal winds decreases its magnitude with depth, implying that the relatively deep zonal winds are stable with time.

The Pioneer and Voyager spacecrafts made flyby visits to the giant planets and conducted snapshot observations. The Galileo and Cassini spacecrafts on the other hand made orbital observations of Jupiter and Saturn respectively, which can be used to track seasonal variations. However, no single spacecraft observation is long enough to explore the temporal variation beyond the seasonal scale on the giant planets due to their long orbital periods. The Cassini observations in 2009–10 and the Voyager observations in 1980–81 both occurred in the northern early spring but were separated by one Saturnian year. Therefore, the combination of observations from Voyager and Cassini makes it possible to examine the non-seasonal variability of the atmosphere over one complete Saturnian year (~29.5 Earth years). Such an exploration will provide important information on the temporal variation of Saturn's atmosphere, which is unique and different from the solar-forced seasonal variation.

Here, we focus on exploring Saturn's atmosphere in the tropical region (i.e., 30°N–30°S), in which the strong atmospheric winds ~400–500 m/s blow from west to east. Our exploration of atmospheric temperature is mainly based on the thermal observations from the infrared spectrometer on Voyager and Cassini^{1,2}. In addition, some independent radio-occultation measurements^{3–6} are used to valid the observations from the infrared spectrometer. Finally, the zonal winds measured by the imaging system on Voyager and Cassini^{7,8} are used as the boundary condition in a modified thermal wind equation^{9–11} to explore the vertical structure of zonal winds in Saturn's upper troposphere (i.e., 50–750 mbar).

In order to explore the temporal variation of Saturn's atmosphere from one Saturnian year to the next, we searched all Cassini observations to select the best data and those as close as possible to one Saturnian year after the Voyager encounter to rule out the seasonal variation on Saturn. The selected observations are listed in Tables S1–S3 in the Supplementary Information. The data processing and the corresponding measurements for these selected observations are also discussed in the Supplementary Information.

Results

Figure 1 displays the tropic temperature in the upper troposphere from the nadir observations recorded by Voyager and Cassini. The zonal-mean temperature from the Infrared Spectrometer (IRIS) on the Voyager (1980–81) and the Composite Infrared Spectrometer (CIRS) on Cassini (2009–10) are displayed in panel A and panel B, respectively. Both of the Voyager/IRIS and Cassini/CIRS temperatures are retrieved from the

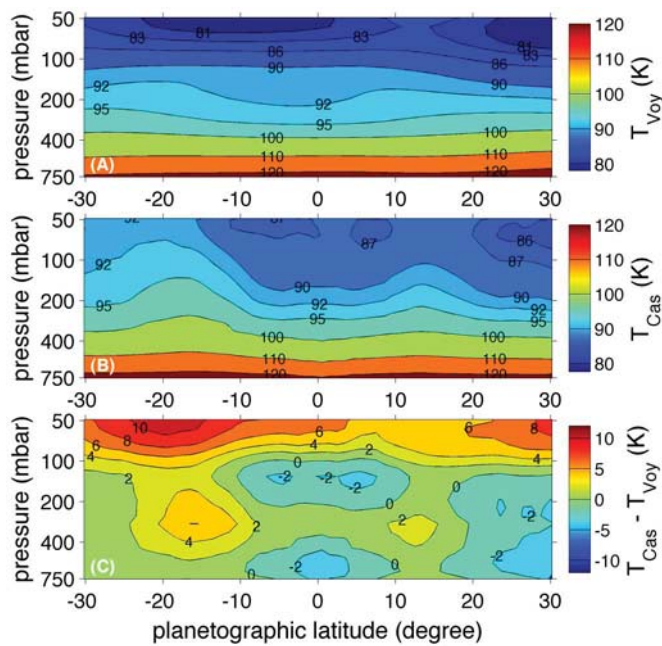


Figure 1 | Temporal variation of Saturn's temperature from the Voyager epoch to the Cassini epoch. (A) Temperature retrieved from the Voyager/IRIS nadir observations (1980–81). (B) Temperature retrieved from the Cassini/CIRS nadir observations (2009–10). (C) Differences of Saturn's temperature between Voyager and Cassini.

spectral measurements within the S(0) and S(1) hydrogen absorption lines with the same retrieval algorithm developed in a previous study¹². The retrieval errors, which are mainly determined by the number of spectra, the signal strength, and the observational

geometry, are estimated as ~ 1 Kelvin for the retrieved temperatures of both Voyager and Cassini^{12,13}. The other errors due to the uncertain optical depth and He/H₂ ratio will probably introduce ~ 2 -Kelvin errors in the retrieved temperature (Section S1 in the Supplementary Information).

Panel C of Fig. 1 is the temporal variation of atmospheric temperature from the Voyager epoch to the Cassini epoch. This panel shows that there is significant tropical warming with a magnitude of ~ 10 Kelvins around the tropopause from one Saturnian year to the next, which is significantly larger than the errors. Below the tropopause, the atmosphere shows a relatively small temporal variation. There is warming of ~ 2 –4 Kelvins around 15° in each hemisphere at the pressure level ~ 300 mbar, which suggests that the temperature knee^{14,15} probably changed its magnitude from the Voyager epoch to the Cassini epoch. At the pressure levels of 150 mbar and 750 mbar, there is cooling of ~ 2 Kelvins around the equator (i.e., 10°S – 10°N), which is close to the retrieval errors.

Figure 2 displays the independent radio-occultation measurements in the epochs of Voyager and Cassini^{5,6}, which are used to validate the temporal variation of atmospheric temperature revealed by the nadir observations from the infrared spectrometers on Voyager and Cassini (Fig. 1). The procedure of computing the temperature profiles from the radio-occultation measurements and the corresponding error estimates are introduced in Section S2 in the Supplementary Information. Figure 2 shows basic consistency of the atmospheric temperature around the tropopause (i.e., 50–70 mbar) between the nadir observations and the occultation measurements, which provides more evidences for the temporal variation of atmospheric temperature revealed by the nadir observations (Fig. 1). There are some discrepancies between the nadir observations and the occultation measurements existing below the pressure level of 70 mbar, but most the discrepancies are smaller than the errors of the corresponding measurements. However, in the Voyager epoch the

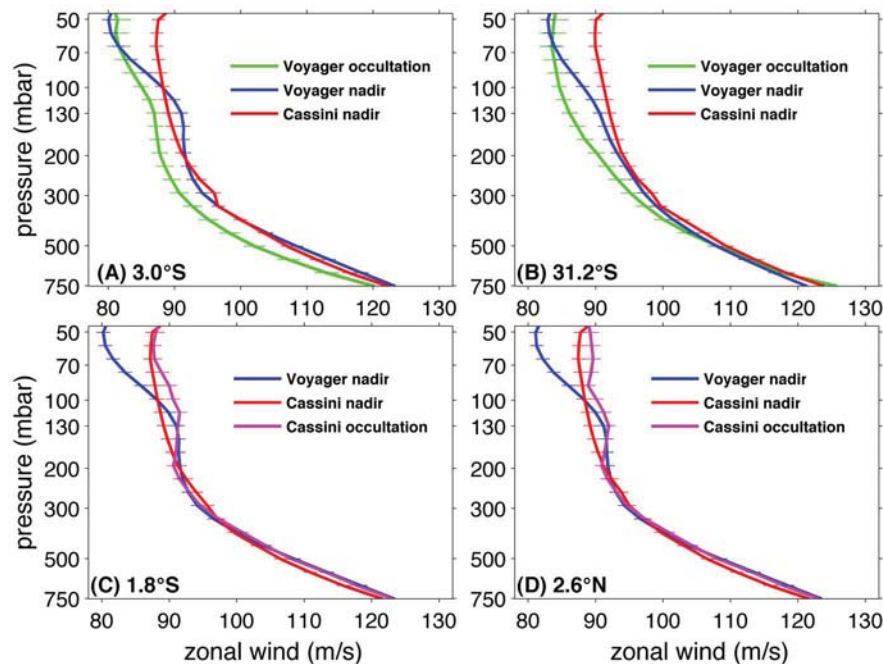


Figure 2 | Comparison between the radio-occultation measurements and the nadir observations in the epochs of Voyager and Cassini.

(A) Temperature comparison at 3.0°S among the radio-occultation measurements by Voyager 1 (1980), the nadir observations by Voyager 1/2 (1980–81), and the nadir observations by Cassini (2009–10). (B) Temperature comparison at 31.2°S among the radio-occultation measurements by Voyager 2 (1981), the nadir observations by Voyager 1/2 (1980–81), and the nadir observations by Cassini (2009–10). (C) Temperature comparison at 1.8°S among the radio-occultation measurements by Cassini (2010), the nadir observations by Voyager 1/2 (1980–81), and the nadir observations by Cassini (2009–10). (D) Temperature comparison at 2.6°N among the radio-occultation measurements by Cassini (2010), the nadir observations by Voyager 1/2 (1980–81), and the nadir observations by Cassini (2009–10). The latitudes shown in this figure are planetographic latitudes.



discrepancies are larger than the corresponding errors in the pressure levels below 100 mbar for the latitudes of 3.0°S (panel A) and 31.2°S (panel B), which are probably due to some unknown systematic errors or underestimated errors. As we discussed in the Supplementary Information (S1), most of the errors in the retrieved temperature are systematic errors. These systematic errors will affect the absolute magnitude of the retrieved temperature, but they do not affect the temperature gradients used in the thermal wind equation and hence do not alter our computations of thermal winds (please refer to S4 in the Supplementary Information).

The significant temporal variation of atmospheric temperature over one Saturnian year is a new discovery. The maximal temporal variation of 10 Kelvins, which is larger than the seasonal variation of a few Kelvins in the same region^{13,16}, suggests that there are strong temporal changes besides the seasonal variation on Saturn. The temporal variation of tropospheric temperature is also different from the semi-annual oscillations^{17,18}, because the semi-annual oscillations were discovered in the middle and high stratosphere of Saturn.

The temperature fields retrieved from the nadir observations (Fig. 1) are further applied to a thermal wind equation to explore the vertical structure of zonal winds, as discussed in some previous studies^{16,19,20}. Here, we used a modified thermal wind equation^{9–11} instead of the classical thermal wind equation^{18–20} to explore the vertical structure of zonal winds in the tropic region of Saturn with emphasizing the temporal variation from the Voyager epoch to the Cassini epoch. In order to integrate the temperature with the modified thermal equation, a boundary level with the known zonal winds is needed. Here, the pressure level of visible clouds at ~ 360 mbar, in which the zonal winds are measured by the Imaging Science Subsystem (ISS) on Voyager and Cassini^{7,8} (Fig. S1 in the Supplementary Information), is used as the boundary level.

Figure 3 shows a comparison of zonal-wind vertical structure between the Voyager epoch and the Cassini epoch. The errors in the computed zonal winds, which are ~ 5 – 30 m/s, are estimated from the uncertainties in the cloud-tracking zonal winds at the boundary level, the uncertainties in the altitude location of the cloud-tracking zonal winds, and the propagating temperature errors in the integration of the modified thermal wind equation (Section S4 in the Supplementary Information). Panel C of Fig. 3 suggests that the zonal winds around 10° latitude in each hemisphere decreased ~ 100 m/s at 50 mbar since the Voyager epoch. The ~ 100 m/s wind variation tilts equatorward from 10° latitude at 50 mbar to 5° latitude at 750 mbar, which suggests that the strong decrease of zonal winds discovered at the cloud level²¹ basically exists in the whole upper troposphere (i.e., 50–750 mbar).

Panel C of Fig. 3 also suggests that the temporal variation of tropic winds decreases its magnitude from 50 mbar to 750 mbar. The temporal variation of zonal winds at different pressure levels is further explored in Fig. 4. Panel A is the comparison of zonal winds at 750 mbar, which shows that the magnitude of the equatorial jet (5°S – 5°N) in the Cassini epoch (~ 450 m/s) is close to that of the equatorial jet in the Voyager epoch (~ 460 m/s). Such a comparison suggests that the 750-mbar zonal winds are relatively stable with time. Panel B of Fig. 4 further displays a comparison of the temporal variation of zonal winds between 360 mbar and 750 mbar, which shows that the temporal variation of zonal winds is stronger at 360 mbar than at 750 mbar. Therefore, the relatively time-constant zonal winds at 750 mbar imply that the atmosphere with pressures greater than 750 mbar probably has relatively small temporal variability.

Besides the temporal stability, the zonal winds at the relatively deep pressure levels also display stability in the vertical direction. The speed of the equatorial jet at 750 mbar (~ 450 – 460 m/s) is close to that of the equatorial jet at 2000 mbar (~ 500 m/s)^{22,23}, which suggests that the equatorial jet does not vary significantly at pressures greater than 750 mbar. The nearly constant equatorial jet from

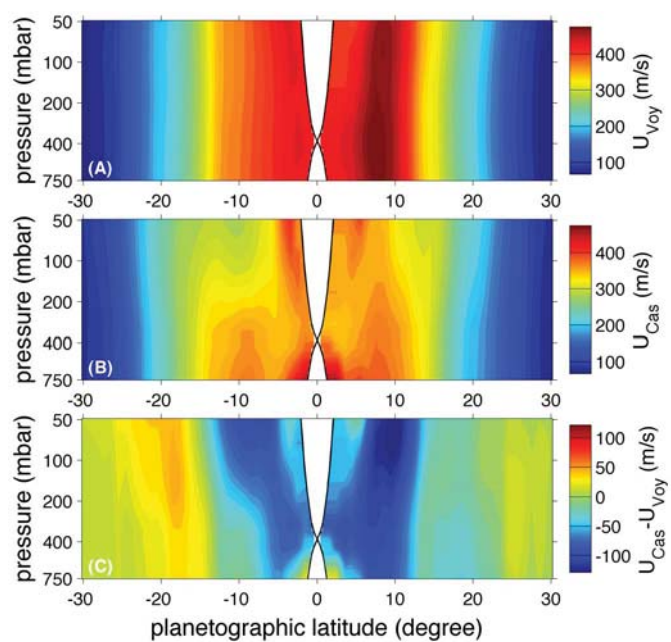


Figure 3 | Temporal variation of zonal winds from the Voyager epoch to the Cassini epoch. The zonal winds in Saturn's upper troposphere (i.e., 50–750 mbar) are computed from the temperature fields by a modified thermal wind equation. The regions within the black lines are left blank because the cylindrical routines of the modified thermal wind equation do not pass the regions. (A) Zonal winds derived from the Voyager/IRIS temperature (1980–81). (B) Zonal winds derived from the Cassini/CIRS temperature (2009–10). (C) Differences of Saturn's zonal winds between Voyager and Cassini.

750 mbar to 2000 mbar provides an observational evidence for a numerical inference on Saturn²⁴ in which zonal winds are suggested to extend from 0.5 bar to ~ 10 bar without significant decay, similar to their observed behavior on Jupiter²⁵.

Discussion

In this study, the combined observations from Voyager and Cassini reveal that the tropical atmospheric temperature around the tropopause warmed more than 10 Kelvins from one Saturnian year (1980–81) to the next (2009–10), which paints a remarkable picture of temporal variation of the thermal fields on Saturn. As the boundary of troposphere and stratosphere, the tropopause plays an important role in planetary atmospheres. The significant warming in the tropopause will modify the atmospheric stratification and stability, and further influence the large-scale dynamics in the upper troposphere. Based on the temperature fields, we also explore the related wind fields, which provide some important information about the temporal stability and vertical structure of zonal winds in the upper troposphere. These important characteristics of the large-scale temperature and wind fields need to be considered in the future studies of the atmospheric system on Saturn.

The 1990 tropical storm²⁶ is one possible driver for the large-scale atmospheric variation on Saturn. But the follow-up studies suggest that such a storm is probably not related to the significant warming around the tropopause (Fig. 1). First, the 1990 giant storm erupted around 5°N ²⁶, which is not consistent with the latitudes (20°S and 30°N) where the maximal warming happened. Second, a model study²⁷ suggests that the 1990 storm mainly developed below the tropopause, which probably did not affect the strong warming around the tropopause. Finally, numerical simulations²⁸ imply that the 1990 storm could not result in the large wind decrease ~ 100 m/s,

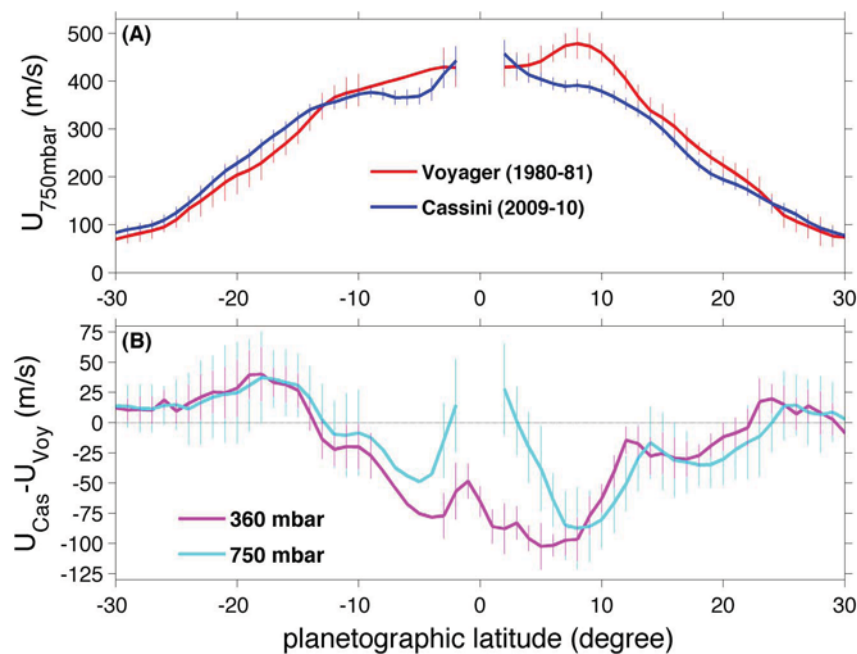


Figure 4 | Comparison of zonal winds between different times and between different pressure levels. (A) Comparison of 750-mbar zonal winds between the Voyager epoch (1980–81) and the Cassini epoch (2009–10). The 750-mbar zonal winds come from the thermal winds shown in Fig. 3. (B) Comparison of temporal variation in the zonal winds between 360 mbar and 750 mbar. The temporal variation of zonal winds at 360 mbar and 750 mbar comes from Fig. S1 and Fig. 3, respectively. There are no Voyager observations for the latitude range of 2.0°S–10°S, which is interpolated from the neighboring measurements. Therefore, there are no error estimates for such a latitude range (2.0°S–10°S) (Section S4 in the Supplementary Information). The gaps around the equator (3°N–3°S) in the 750-mbar profiles are due to the integration routines of the modified thermal wind equation.

which is related to the temperature changes. Even though the 1990 storm is not directly related to the temporal variation discussed in this paper, it is possible that some dynamical changes induced by the 1990 storm and other storms play roles in the large-scale atmospheric variation from Voyager to Cassini.

In addition, the wave activity is the other possible driver for the large-scale atmospheric variation on Saturn. Waves are active on Saturn²⁹. In the tropical region, we just identified a planetary-scale wave in the stratosphere¹¹. In addition, the thermal maps from the Cassini/CIRS show some wavelike structures in the tropic region of troposphere (Fig. S4 in the Supplementary Information). Atmospheric waves can generate the inter-annual variability in the wind and temperature fields in the stratospheres of Earth³⁰ and Jupiter³¹. It is possible that the waves also play an important role in driving the large-scale variation in Saturn's atmosphere from one year to the next.

Finally, the energy budget affects the thermal structure on planets. Therefore, the exploration of energy budget provides one more perspective to explore the temporal variation of the thermal structure and the corresponding dynamical fields. Saturn's energy budget is mainly determined by the absorbed solar energy, emitted thermal energy, and internal heat. The time scale of the internal heat on the giant planets is generally thought to be much longer than a Saturnian year³², but the other two energy components (i.e., the absorbed solar energy and the emitted thermal energy) are variable on the time scale of Saturnian year. Our related study³³ revealed that Saturn's emitted power varied from the Voyager epoch to the Cassini epoch. In addition, Saturn's absorbed solar energy probably changes with time because of the varying total solar flux³⁴ and the varying albedo due to the temporal variation of clouds^{35,36}. We are exploring the temporal variation of the absorbed solar energy and hence the temporal variation of the energy budget on Saturn. Such a study will help us examine the role of energy budget in the temporal variation of atmospheric temperature revealed in this study.

Methods

Our results are based on the measurements of zonal winds and atmospheric temperature on Saturn in the two epochs (i.e., Voyager (1980–81) and Cassini (2009–10)). In addition, a modified thermal wind equation^{9–11} is applied to explore the vertical structure of zonal winds. In this section, we introduce the methods of measuring and computing the zonal winds and atmospheric temperature on Saturn. The full details of the data sets and the corresponding methods are included in the Supplementary Information.

The retrieval of Saturn's atmospheric temperature (Fig. 1) is mainly based on the infrared spectra recorded by the Infrared Spectrometer (IRIS) on Voyager⁴ and the Composite Infrared Spectrometer (CIRS) on Cassini². The process of retrieving atmospheric temperature is based on a retrieval algorithm developed by our co-authors and described in our previous study¹². We also put some introduction of the retrieval algorithm in the Supplementary Information (Section S1). The retrieval errors of the retrieved temperature are estimated by considering these dominant factors affecting the retrieval, which include signal strength, varying optical depth, and the helium volume mixing ratio (please refer to Section S1 in the Supplementary Information for the detailed discussion). To validate the retrieved temperature from the infrared spectrometers, we also use some independent observations from the radio-occultation measurements (Fig. 2) by Voyager (1980–81) and Cassini (2010), which come from previous analyses^{5,6}. The detailed information of the previous analysis and the corresponding error estimates are put in Section S2 in the Supplementary Information.

The measurements of Saturn's zonal winds (Fig. S1) are based on the observations from the Imaging Science Subsystem (ISS) on Voyager⁷ and Cassini⁸, which are described in Section 3 of the Supplementary Information. The basic method of measuring zonal winds is to track the visible cloud features on the ISS images. The errors of wind measurements are estimated by the standard deviation of the wind measurements in each latitude bin. Our discussion in Section 3 of the Supplementary Information shows that the other possible sources of errors in the wind measurements, which include the errors due to the navigation procedure and the uncertainty related to locating cloud features when conducting the cloud-tracking wind measurements, are negligible to the standard deviation of the wind measurements.

The vertical structure of Saturn's zonal winds (Fig. 3) are based on the integration of our modified thermal wind equation, which was described and validated in our previous studies^{9–11}. The basic methodology is to integrate the thermal wind equation with the retrieved temperature from the Voyager/IRIS and the Cassini/CIRS (Fig. 1) from a pressure level with known zonal winds. Such a pressure level is set as the pressure level in which the cloud-track zonal winds are measured from the ISS images (Section 3 of the Supplementary Information). The errors in the computed zonal winds (Fig. S5) from our modified thermal wind equation are estimated by the combination of three dominant error sources, which include the uncertainties in the



cloud-tracking zonal winds (Fig. S2), the uncertainties in the altitude location of the cloud-tracking winds (Figs. S3), and the uncertainty related to the errors in the retrieved temperature (Fig. S4). We discussed the three dominant error sources in Section 4 of the Supplementary Information, and the corresponding error estimates are used in Fig. 4 in the text.

1. Hanel, R. *et al.* Infrared spectrometer for Voyager. *Applied Optics* **19**, 1391–1400 (1980).
2. Flasar, F. M. *et al.* Exploring the Saturn system in the thermal infrared: the composite infrared spectrometer. *Space Sci. Rev.* **115**, 169–297 (2004).
3. Tyler, G. L. *et al.* Radio science investigation of the Saturn system with Voyager 1: preliminary results. *Science* **212**, 201–206 (1981).
4. Tyler, G. L. *et al.* Radio science with Voyager 2 at Saturn–Atmosphere and ionosphere and the masses of Minimas, Tethys, and Lapetus. *Science* **215**, 553–558 (1982).
5. Lindal, G. F., Sweetnam, D. N. & Eshleman, V. R. The atmosphere of Saturn: an analysis of the Voyager radio occultation measurements. *Astron. J.* **90**, 1136–1146 (1985).
6. Schinder, P. J. *et al.* Saturn's equatorial oscillation: evidence of descending thermal structure from Cassini radio occultations. *Geophys. Res. Lett.* **38**(8), L08205 (2011).
7. Smith, B. A. *et al.* Voyager imaging experiment. *Space Sci. Rev.* **21**, 103–127 (1977).
8. Porco, C. C. *et al.* Cassini Imaging Science: Instrument characteristics and anticipated scientific investigations at Saturn. *Space Sci. Rev.* **115**, 363–497 (2004).
9. Flasar, F. M. *et al.* Titan's atmospheric temperatures, winds, and composition. *Science* **308**, 975–978 (2005).
10. Li, L., Conrath, B. J., Flasar, F. M. & Cierasch, P. J. Revisit of the thermal wind equation: application to planetary atmospheres. *EOS Transactions American Geophysical Union* **88**, P41A–0208 (2007).
11. Li, L. *et al.* Strong jet and a new thermal wave in Saturn's equatorial stratosphere. *Geophys. Res. Lett.* **35**(23), L23208 (2008).
12. Conrath, B. J., Gierasch, P. J. & Ustinov, E. A. Thermal structure and para hydrogen fraction on the outer planets from Voyager IRIS measurements. *Icarus* **135**, 501–517 (1998).
13. Fletcher, L. N. *et al.* Seasonal Change on Saturn from Cassini/CIRS Observations, 2004–2009. *Icarus* **208**, 337–352 (2010).
14. Hanel, R. *et al.* Infrared observations of the Saturnian system from Voyager 1. *Science* **212**, 192–200 (1982).
15. Fletcher, L. N. *et al.* Characterising Saturn's vertical temperature structure from Cassini/CIRS. *Icarus* **189**, 457–478 (2007).
16. Conrath, B. J. & Pirraglia, J. A. Thermal structure of Saturn from Voyager infrared measurements: implications for atmospheric dynamics. *Icarus* **53**, 286–292 (1983).
17. Fouchet, T. *et al.* An equatorial oscillation in Saturn's middle atmosphere. *Nature* **453**, 200–202 (2008).
18. Orton, G. S. *et al.* Semi-annual oscillations in Saturn's low-altitude stratospheric temperatures. *Nature* **453**, 196–199 (2008).
19. Flasar, F. M. *et al.* Temperatures, winds, and composition in the Saturnian system. *Science* **307**, 1247–1251 (2005).
20. García-Melendo, E., Pérez-Hoyos, S., Sánchez-Lavega, A. & Hueso, R. Saturn's zonal wind profile in 2004–2009 from Cassini ISS images and its long-term variability. *Icarus* **215**, 62–74 (2011).
21. Sánchez-Lavega, A., Pérez-Hoyos, S., Rojas, J. F., Hueso, R. & French, R. G. A strong decrease in Saturn's equatorial jet at cloud level. *Nature* **423**, 623–625 (2003).
22. Baines, K. H., Momary, T. W. & Roos-Serote, M. The deep winds of Saturn: First measurements of the zonal wind field near the two-bar level. *Bull. Am. Astron. Soc.* **37**, 658 (2005).
23. Choi, D. S., Showman, A. P. & Brown, R. H. Cloud features and zonal wind Measurements of Saturn's atmosphere as observed by Cassini/VIMS. *J. Geophys. Res.* **114**, E04007 (2009).
24. Sánchez-Lavega, A. *et al.* Deep winds beneath Saturn's upper clouds from a seasonal long-lived planetary-scale storm. *Nature* **475**, 71–74 (2011).
25. Atkinson, D. H., Pollack, J. B. & Seiff, A. The Galileo Probe Doppler wind experiment: measurement of the deep zonal winds on Jupiter. *J. Geophys. Res.* **103**, 22911–22928 (1998).
26. Sánchez-Lavega, A. *et al.* The great white spot and disturbance in Saturn's equatorial atmosphere during 1990. *Nature* **353**, 397–401 (1991).
27. Acarreta, J. R. & Sánchez Lavega, A. Vertical cloud structure in Saturn's 1990 equatorial storm. *Icarus* **137**, 24–33 (1999).
28. Sayanagi, K. M. & Showman, A. P. Effects of a large convective storm on Saturn's equatorial jet. *Icarus* **187**, 520–539 (2007).
29. Achterberg, R. K. & Flasar, F. M. Planetary-scale thermal waves in Saturn's upper troposphere. *Icarus* **119**, 350–359 (1996).
30. Lindzen, R. S. & Holton, J. R. A theory of quasi-biennial oscillation. *J. Atmos. Sci.* **25**, 1095–1107 (1968).
31. Friedson, A. J. New observations and modeling of a QBO-like oscillation in Jupiter's stratosphere. *Icarus* **137**, 34–55 (1999).
32. Flasar, F. M. Gravitational energy sources in Jupiter. *Astrophys. J.* **186**, 1097–1106 (1973).
33. Li, L. *et al.* Emitted power of Saturn. *J. Geophys. Res.* **115**, E11002 (2010).
34. Lean, J., Rottman, G., Harder, J. & Kopp, G. SORCE contributions to new understanding of global change and solar variability. *Sol. Phys.* **230**, 27–53 (2005).
35. Karkoschka, E. & Tomasko, M. Saturn's vertical and latitudinal cloud structure 1991–2004 from HST imaging in 30 filters. *Icarus* **179**, 195–221 (2005).
36. Pérez-Hoyos, S., Sánchez-Lavega, A., French, R. G. & Rojas, J. F. Saturn's cloud structure and temporal evolution from ten years of Hubble Space Images (1994–2003). *Icarus* **176**, 155–174 (2005).

Acknowledgements

NASA Cassini Data Analysis and Outer Planets Research Programs funded this work. We acknowledge the teams of Voyager (IRIS and ISS) and Cassini (CIRS and ISS) for providing the data sets. We also thank the anonymous reviewers for their constructive suggestions.

Author contributions

L.L. measured the zonal winds from the Cassini ISS observations, computed the thermal winds, and conceived the overall research. R.K.A. retrieved the atmospheric temperature from the Cassini CIRS observations. P.J.G. and B.J.C. provided the data of atmospheric temperature retrieved from the Voyager IRIS observations. M.A.S. and X.J. took part in active discussions and provided constructive suggestions during every phase of this study. L.L., R.K.A., B.J.C., P.J.G., M.A.S., A.A.S.-M., C.A.N., G.S.O., F.M.F., X.J., K.H.B., R.M.-J., A.P.I., A.R.V., A.D.D.G., R.A.W. and S.P.E. participated in the analysis and interpretation of the results and the writing of the manuscript.

Additional information

Supplementary information accompanies this paper at <http://www.nature.com/scientificreports>

Competing financial interests: The authors declare no competing financial interests.

How to cite this article: Li, L. *et al.* Strong Temporal Variation Over One Saturnian Year: From Voyager to Cassini. *Sci. Rep.* **3**, 2410; DOI:10.1038/srep02410 (2013).



This work is licensed under a Creative Commons Attribution-NonCommercial-NoDerivs 3.0 Unported license. To view a copy of this license, visit <http://creativecommons.org/licenses/by-nc-nd/3.0>